

Article

Synthesis, Crystal Structure, Photoluminescence Properties and Antibacterial Activity of a Zn(II) Coordination Polymer Based on a Paddle-Wheel Cluster

Qingguo Meng¹, Lintong Wang¹, Dongfang Wang², Jianjian Yang¹, Chen Yue¹ and Jitao Lu^{1,*}

¹ College of Chemical Engineering and Environmental Chemistry, Weifang University, Weifang 261061, China; mengqg@wfu.edu.cn (Q.M.); wanglt6408@163.com (L.W.); yangjianjian9@163.com (J.Y.); wfuyuechen@163.com (C.Y.)

² College of Bioengineering, Weifang University, Weifang 261061, China; wangdf@wfu.edu.cn

* Correspondence: lujitao@foxmail.com

Academic Editor: Shujun Zhang

Received: 15 March 2017; Accepted: 13 April 2017; Published: 17 April 2017

Abstract: A binuclear Zn(II) complex of formula $\{[\text{Zn}(\text{BCPPO})\text{H}_2\text{O}]\cdot 3\text{C}_2\text{H}_5\text{OH}\}_n$ (**1**) [H_2BCPPO = Bis 4-carboxyphenyl phenyl phosphine oxide] has been synthesized and structurally characterized by single crystal X-ray diffraction, Powder X-ray diffraction (PXRD), Thermogravimetric analysis (TG), Elemental analysis (EA) and Infrared spectroscopy (IR). As revealed by the single crystal X-ray diffraction, in the binuclear Zn(II) complex, two paddle-wheel-type Zn_2 units were connected by four BCPPO ligands to form one-dimensional chains. Their antibacterial activity was evaluated by using a minimal bactericidal concentration (MBC) benchmark. The binuclear Zn(II) complex shows excellent and long-term antibacterial activity against *Escherichia coli* and *Staphylococcus aureus*. In addition, the Photoluminescence properties of the binuclear Zn(II) complex was also investigated.

Keywords: Bis 4-carboxyphenyl phenyl phosphine oxide; coordination polymers; antibacterial activity; photoluminescence properties

1. Introduction

In recent years, coordination polymers (CPs), which are assembled by metal ions/clusters and organic ligands, have attracted considerable attention owing to their fascinating structural topologies and potential applications in gas storage, separation, drug delivery, chemical absorption, luminescence, electronics, catalysis and their biological activity [1–10]. In particular, the luminescent coordination polymers have become an active topic of investigation due to the various applications in chemical sensors, photochemistry and electroluminescent display [11–14]. General d^{10} transition metal are particularly remarkable candidates in the construction of photoluminescence materials because the metal is hard to oxidize or reduce [15–17].

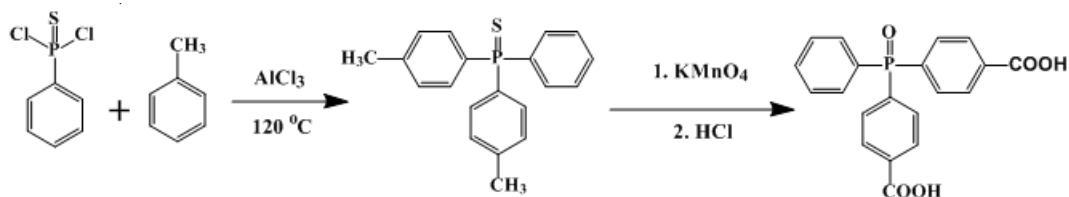
In the past decades, plenty of people have suffered from diseases caused by unsafe drinking water and food containing bacteria such as *Escherichia coli*, *Staphylococcus aureus* and *Bacillus subtilis*. The traditional low molecular weight antibacterial materials have many disadvantages, such as toxicity to the environment and short-term antibacterial activity. Hence, there is an urgent need for the development of effective antibacterial materials. Among chemical disinfectants, metal/metal oxide nanoparticulate systems, as well as coordination polymers (CPs), have attracted increasing attention because CPs can be easy recycled to minimize the environmental problems and CPs with high surface area show more active sites resulting in excellent antibacterial activity [18–21].

With the above issues in mind, in order to design and synthesize coordination polymers and explore the potential application in photochemistry and antibacterial, in the present work, a binuclear Zn(II) complex of formula $\{[Zn(BCPPO)H_2O] \cdot 3C_2H_5OH\}_n$ (**1**) [BCPPO = Bis 4-carboxyphenyl phenyl phosphine oxide] has been synthesized and structurally characterized by single crystal X-ray diffraction; powder X-ray diffraction (PXRD), Figure S1; Elemental analysis (EA) and Infrared Spectroscopy (IR), Figure S2; thermogravimetric analysis (TG), Figure S3. The complex **1** shows excellent and long-term antibacterial activity against *Escherichia coli* and *Staphylococcus aureus*. In addition, the Photoluminescence properties of the binuclear Zn(II) complex was also investigated.

2. Experimental Section

2.1. Materials and Methods

Bis 4-carboxyphenyl phenyl phosphine oxide was prepared (Scheme 1) according to the published procedure [22]. All the other chemicals were of reagent grade and were used as commercially obtained without further purification. Elemental analyses (for C or H) were carried out on an Elementar Vario EL III elemental analyzer (Hanau, Germany). PXRD measurements were performed with a Bruker AXS D8 Advance instrument (Karlsruhe, Germany). The FT-IR spectra were recorded in the range $4000\text{--}400\text{ cm}^{-1}$ on a Nicolet 330 FTIR Spectrometer (Nicolet Instrument Inc., Madison, WI, USA) using the KBr pellet method. TGA experiments were performed using a PerkinElmer TGA 7 instrument (PerkinElmer, Billerica, MA, USA, heating rate of $10\text{ }^\circ\text{C min}^{-1}$, nitrogen stream).



Scheme 1. The synthesis procedure of H₂BCPPO.

2.2. Synthesis of $\{[Zn(BCPPO)H_2O] \cdot 3C_2H_5OH\}_n$ (**1**)

A mixture of Bis 4-carboxyphenyl phenyl phosphine oxide (0.015 mmol, 5 mg) and $Zn(NO_3)_2 \cdot 6H_2O$ (0.10 mmol, 30 mg) were dissolved in 4 mL of mixed solvents of DMF/ C_2H_5OH/H_2O (2:1:1). After ultrasounding at room temperature for 10 min. The glass tube was sealed and placed in an oven and slowly heated to $75\text{ }^\circ\text{C}$ from room temperature in 10 h, kept at $75\text{ }^\circ\text{C}$ for 72 h, and then slowly cooled to $30\text{ }^\circ\text{C}$. Colorless block-shaped crystals suitable for X-ray diffraction analysis were separated by filtration with the yield of 0.029 g, 49.6% (based on zinc). Anal. Calc. (found) for $C_{26}H_{33}O_9PZn$: C, 53.30 (53.34); H, 5.68 (5.71). IR (KBr): ν (cm^{-1}) = 3435 (s), 1650 (s), 1556 (s), 1495 (w), 1404 (s), 1167 (s), 1119 (s), 1018 (m), 848 (w), 777 (m), 734 (s), 700 (m), 564 (m), 501 (m), 437 (m).

2.3. X-ray Crystallography

Single crystal of the complex **1** with appropriate dimensions was chosen under an optical microscope and quickly coated with high vacuum grease before being mounted on a glass fiber for data collection. Data were collected on a Bruker Apex II Image Plate single-crystal diffractometer with graphite-monochromated Mo K α radiation source ($k = 0.71073\text{ \AA}^\circ$) operating at 50 kV and 30 mA for complex **1**. All absorption corrections were applied using the multi-scan program SADABS [23]. In all cases, the highest possible space group was chosen. The structure was solved by direct methods using SHELXS-97 [24] and refined on F^2 by full-matrix least-squares procedures with SHELXL-97 [25]. Atoms were located from iterative examination of difference F-maps following least squares refinements of the earlier models. Hydrogen atoms were placed in calculated positions and included as riding atoms with isotropic displacement parameters 1.2 times U_{eq} of the attached C

atoms. All structures were examined using the Addsym subroutine of PLATON [26] to assure that no additional symmetry could be applied to the models. The crystallographic details of complex 1 are summarized in Table 1. Selected bond lengths and angles for complex 1 are collected in Table 2.

Table 1. Crystal data for complex 1.

Empirical Formula	C ₂₀ H ₁₅ O ₆ PZn
Formula weight	447.66
Temperature (K)	293(2)
Crystal system	monoclinic
Space group	C2/c
<i>a</i> (Å)	23.5029(6)
<i>b</i> (Å)	10.2695(3)
<i>c</i> (Å)	17.9148(5)
α (°)	90
β (°)	100.861(3)
γ (°)	90
Volume (Å ³)	4246.52(19)
<i>Z</i>	8
ρ_{calc} (mg/mm ³)	1.400
μ (mm ⁻¹)	1.263
<i>F</i> (000)	1824.0
Index ranges	$-20 \leq h \leq 27, -12 \leq k \leq 12, -21 \leq l \leq 20$
Reflections collected	8476
Independent reflections	3735 [Rint = 0.0300, Rsigma = 0.0442]
Data/restraints/parameters	3735/0/254
Goodness-of-fit on <i>F</i> ²	1.072
Final R indexes [<i>I</i> ≥ 2σ (<i>I</i>)]	<i>R</i> ₁ = 0.0436, <i>wR</i> ₂ = 0.1190
Final R indexes [all data]	<i>R</i> ₁ = 0.0554, <i>wR</i> ₂ = 0.1257
Largest diff. peak/hole (e Å ⁻³)	0.60/−0.34

Table 2. Selected bond lengths (Å) and angles (°) for complex 1.

Zn1-O2 ¹	2.038(3)	Zn1-O1w	1.978(3)	Zn1-O1	2.021(3)
Zn1-O4 ²	2.035(3)	Zn1-O3 ³	2.048(2)	O2 ¹ -Zn1-O3 ²	87.85(13)
O1w-Zn1-O2 ¹	98.41(13)	O1w-Zn1-O1	103.08(13)	O1w-Zn1-O4 ³	101.13(12)
O1w-Zn1-O3 ²	100.73(12)	O1-Zn1-O2 ¹	158.51(13)	O1-Zn1-O4 ³	87.59(12)
O1-Zn1-O3 ²	87.54(12)	O4 ³ -Zn1-O2 ¹	88.93(12)	O4 ³ -Zn1-O3 ²	158.15(11)

Symmetry codes: ¹ 2 − *X*, 3 − *Y*, 1 − *Z*; ² 1/2 + *X*, 1/2 + *Y*, +*Z*; ³ 3/2 − *X*, 5/2 − *Y*, 1 − *Z*.

2.4. Antibacterial Activity

The complex was dissolved in N, N-dimethylformamide (DMF) and tested against two reference strains for antibacterial activity, by use of a modified version of the twofold serial dilution method [27] in which the concentration of the complex was repeatedly reduced by half in sterile culture medium containing broth as nutrient. The strains were incubated for 16 h in culture medium at a constant temperature of 37 °C after being activated then added to test tubes containing the complex. Readings were taken after incubation for 24 h at 37 °C. All other test conditions were standardized. Turbidity in all tubes was estimated visually, and the lowest drug concentration inhibiting growth was defined as the minimum inhibitory concentration (MIC). After continuous incubation for 48 h, the minimal bactericidal concentration (MBC) was also defined.

X-ray Powder Diffraction Analyses; IR Spectra; Thermogravimetric Analyse; The solid state photoluminescence spectra of complex 1 and H₂BCPPO at room temperature. CCDC 1055678 contains the supplementary crystallographic data for this paper. These data can be obtained free of charge from The Cambridge Crystallographic Data Centre via http://www.ccdc.cam.ac.uk/data_request/cif.

3. Results and Discussion

3.1. Structural Description of $\{[Zn(BCPPO)H_2O] \cdot 3C_2H_5OH\}_n$ (**1**)

A single-crystal X-ray crystallographic study reveals that the Zn(II) coordination polymer crystallizes in the space group $C2/c$ with Z value of 8. As can be seen from Figure 1, complex **1** is a one-dimensional chain consisting of paddle-wheel $\{Zn_2(COO)_4\}$ clusters and BCPPO ligands. The coordination environment of the Zn(II) ion is shown in Figure 2. The Zn(II) ion is five-coordinate and displays a typical ZnO_5 square-pyramidal coordination geometry. Each Zn(II) ion bonds to one oxygen donor's atom from one water [$Zn1-O1w$ 1.978(3) Å] in the apical position, and four carboxylate oxygen donor atoms from four BCPPO ligands [$Zn1-O1$ 2.021(3) Å, $Zn1-O2$ 2.038(3) Å, $Zn1-O3$ 2.048(2) Å, $Zn1-O4$ 2.035(3) Å] in the basal plane. Two zinc ions are bridged by four carboxylate groups to form the paddle-wheel binuclear zinc carboxylate clusters $\{Zn_2(COO)_4\}$ with Zn-Zn distances of 2.9822(8) Å. The $\{Zn_2(COO)_4\}$ clusters are further linked by four BCPPO ligands to create a one-dimensional chain, Figure 1. It is worth pointing out that the tetrahedral geometry at P provides an organic building block that greatly favors the formation of 3-dimensional polymers. However, in complex **1**, the $P=O$ unit of BCPPO does not coordinate with any Zn(II) ion, resulting in the formation the one-dimensional chain.

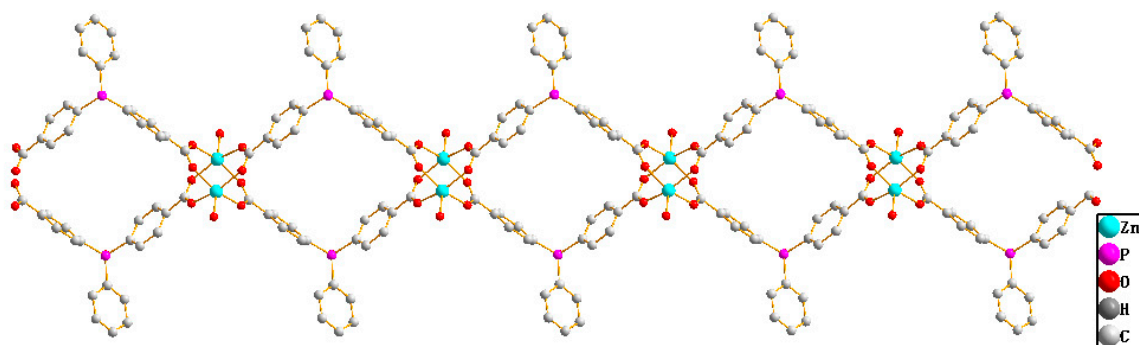


Figure 1. The one-dimensional chain structure of complex **1**.

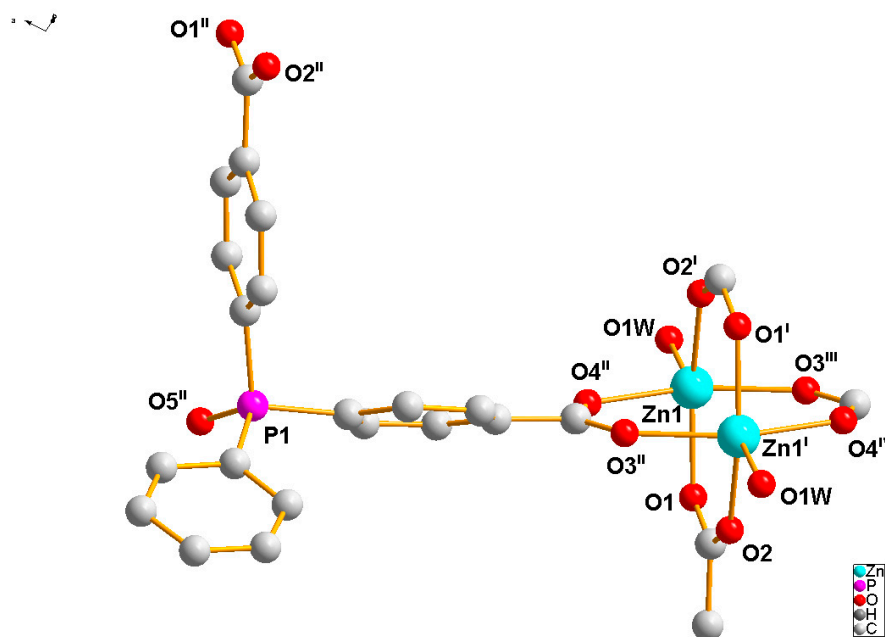


Figure 2. The coordination environment of Zn(II) center of complex **1**.

3.2. Photoluminescence Properties

In order to demonstrate the potential application of the complex, the photoluminescence spectra of complex **1** and H₂BCPPO were investigated in the solid state at room temperature. As shown in Figure S4, the ligand displays emission peak at 429 nm upon excitation at 396 nm, which can be attributed to the intraligand and $\pi^*-\pi$ or $\pi-n$ electronic transition. However, the emission peak of complex **1** appears at 447 nm with 18 nm of red shift when compared with the H₂BCPPO ligand, which is probably assigned to a mixture characteristic of intraligand and ligand-to-ligand charge transition as Zn(II) ion belongs to d¹⁰ electronic configurations and is difficult to oxidize or reduce [28].

3.3. Antibacterial Activity

In order to explore the potential application of complex **1** in an antibacterial situation, the antibacterial activity of the complex **1** was assayed against *Escherichia coli*, and *Staphylococcus aureus*. The inhibition zone test graphs of H₂BCPPO, DMF and complex **1** against *Escherichia coli* and *Staphylococcus aureus* are shown in Figure 3. As can be seen, H₂BCPPO and DMF did not show antibacterial activity; however, complex **1** had some antibacterial activity to both of the two model bacterial strains, which means that the antibacterial activity has relations with complex **1**. The twofold serial dilution method was employed to further investigate the antibacterial activity of the complex **1**. The results indicated that the minimum bactericidal concentration of complex **1** against *Escherichia coli*, and *Staphylococcus aureus* is 0.0625 and 0.125 mg/mL, respectively, which are similar to those reported previously for Zn(II) complexes [29,30]. Therefore, complex **1** has potential applications as a broad-spectrum antibacterial agent.

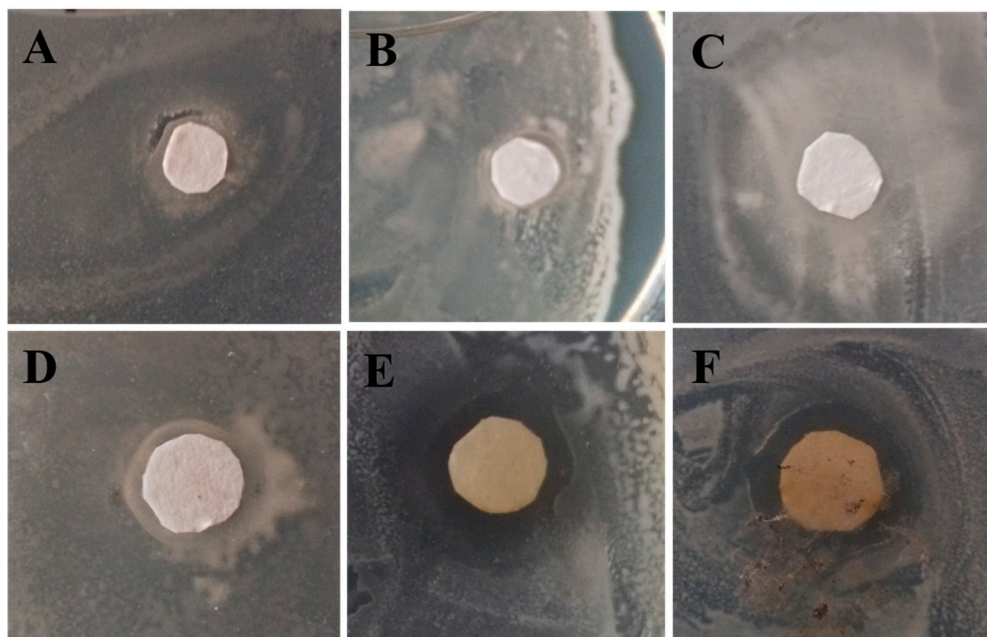


Figure 3. The inhibition zone test graphs of H₂BCPPO (A), N, N-dimethylformamide (DMF) (C), complex **1** (E) against *Escherichia coli* and H₂BCPPO (B), DMF (D), complex **1** (F) against *Staphylococcus aureus*, respectively.

4. Conclusions

In summary, a dinuclear Zn(II) complex has been synthesized and structurally characterized. As revealed by the single crystal X-ray diffraction, in the dinuclear Zn(II) complex, two paddle-wheel-type Zn₂ units were connected by four BCPPO ligands to form one-dimensional chains. The dinuclear Zn(II) complex shows excellent and long-term antibacterial activity against

Escherichia coli and *Staphylococcus aureus*. In addition, the photoluminescence spectra show that the dinuclear Zn(II) complex could be useful for a wide range of photochemistry and electroluminescent display applications.

Supplementary Materials: The following are available online at <http://www.mdpi.com/2073-4352/7/4/112/s1>, Figure S1: The powder XRD patterns and the simulated one from the single-crystal diffraction data for complex 1; Figure S2: FT-IR spectra of complex 1; Figure S3: TG curve of complex 1; Figure S4: The solid state photoluminescence spectra of complex 1 and H₂BCPPO at room temperature.

Acknowledgments: We gratefully thank the financial support of Shandong Provincial Natural Science Foundation (ZR2015BM005), the NSF of China (Grant No. 21301129), and the China Postdoctoral Science Foundation (2015M572093).

Author Contributions: Jitao Lu and Qingguo Meng conceived and designed the experiments; Dongfang Wang and Chen Yue performed the experiments; Lintong Wang and Jianjian Yang analyzed the data; Jitao Lu wrote the paper.

Conflicts of Interest: The authors declare no conflict of interest.

References

1. Suh, M.P.; Park, H.J.; Prasad, T.K.; Lim, D.W. Hydrogen Storage in Metal-Organic Frameworks. *Chem. Rev.* **2012**, *112*, 782–835. [[CrossRef](#)] [[PubMed](#)]
2. Zhou, H.C.; Long, J.R.; Yaghi, O.M. Introduction to Metal-Organic Frameworks. *Chem. Rev.* **2012**, *112*, 673–674. [[CrossRef](#)] [[PubMed](#)]
3. Sumida, K.; Rogow, D.L.; Mason, J.A.; McDonald, T.M.; Bloch, E.D.; Herm, Z.R.; Bae, T.H.; Long, J.R. Carbon Dioxide Capture in Metal-Organic Frameworks. *Chem. Rev.* **2012**, *112*, 724–781. [[CrossRef](#)] [[PubMed](#)]
4. Wei, Z.; Gu, Z.-Y.; Arvapally, R.K.; Chen, Y.-P.; McDougald, R.N., Jr.; Lvy, J.F.; Yakovenko, A.A.; Feng, D.; Omary, M.A.; Zhou, H.C. Rigidifying Fluorescent Linkers by Metal-Organic Framework Formation for Fluorescence Blue Shift and Quantum Yield Enhancement. *J. Am. Chem. Soc.* **2014**, *136*, 8269–8276. [[CrossRef](#)] [[PubMed](#)]
5. Trzop, E.; Zhang, D.; Pñiro-Lopez, L.; Valverde-Muñz, F.J.; Muñz, M.C.; Palatinus, L.; Guerin, L.; Cailleau, H.; Real, J.A.; Collet, E. First Step towards a Devil's Staircase in Spin-Crossover Materials. *Angew. Chem. Int. Ed.* **2016**, *55*, 8675–8679. [[CrossRef](#)] [[PubMed](#)]
6. Fei, H.; Shin, J.; Meng, Y.S.; Adelhardt, M.; Sutter, J.; Meyer, K.; Cohen, S.M. Reusable Oxidation Catalysis Using Metal-Monocatecholato Species in a Robust Metal-Organic Framework. *J. Am. Chem. Soc.* **2014**, *136*, 4965–4973. [[CrossRef](#)] [[PubMed](#)]
7. Xue, C.C.; Zhang, H.Y.; Zhang, D.P. Synthesis, Crystal Structure, and Magnetic Characterization of Two Manganese Schiff-Base-Containing Complexes. *Russ. J. Coord. Chem.* **2017**, *43*, 260–266.
8. Meng, Q.; Xin, X.; Zhang, L.; Dai, F.; Wang, R.; Sun, D. A multifunctional Eu MOF as a fluorescent pH sensor and exhibiting highly solvent-dependent adsorption and degradation of rhodamine B. *J. Mater. Chem. A* **2015**, *3*, 24016–24021. [[CrossRef](#)]
9. Zhu, Q.L.; Xu, Q. Metal-organic framework composites. *Chem. Soc. Rev.* **2014**, *43*, 5468–5512. [[CrossRef](#)] [[PubMed](#)]
10. Shi, J.; Xue, C.; Kong, L.; Zhang, D. Three 1D cyanide-bridged M(Ni, Pd, Pt)-Mn(II) coordination polymer: Synthesis, crystal structure and magnetic properties. *Acta Chim. Slov.* **2017**, *64*, 215–220. [[PubMed](#)]
11. Sun, D.; Yan, Z.; Liu, M.; Xie, H.; Yuan, S.; Lu, H.; Feng, S.; Sun, D. Three- and Eight-Fold Interpenetrated ThSi₂ Metal-Organic Frameworks Fine-Tuned by the Length of Ligand. *Cryst. Growth Des.* **2012**, *12*, 2902–2907. [[CrossRef](#)]
12. Sun, D.; Xu, H.; Yang, C.; Wei, Z.; Zhang, N.; Huang, R.; Zheng, L. Encapsulated Diverse Water Aggregates in Two Ag(I)/4,4'-Bipyridine/Dicarboxylate Hosts: 1D Water Tape and Chain. *Cryst. Growth Des.* **2010**, *10*, 4642–4649. [[CrossRef](#)]
13. Wang, S.; Xiong, S.; Wang, Z.; Du, J. Rational Design of Zinc-Organic Coordination Polymers Directed by N-Donor Co-ligands. *Chem. Eur. J.* **2011**, *17*, 8630–8642. [[CrossRef](#)] [[PubMed](#)]
14. Zhang, L.; Kang, Z.; Xin, X.; Sun, D. Metal-organic frameworks based luminescent materials for nitroaromatics sensing. *CrystEngComm* **2016**, *18*, 193–206. [[CrossRef](#)]

15. Rao, X.; Song, T.; Gao, J.; Cui, Y.; Yang, Y.; Wu, C.; Chen, B.; Qian, G. A highly sensitive mixed lanthanide metal-organic framework self-calibrated luminescent thermometer. *J. Am. Chem. Soc.* **2013**, *135*, 15559–15564. [[CrossRef](#)] [[PubMed](#)]
16. Zang, S.; Cao, L.; Liang, R.; Hou, H.; Mak, T. Divalent Zinc, Cobalt, and Cadmium Coordination Polymers of a New Flexible Trifunctional Ligand: Syntheses, Crystal Structures, and Properties. *Cryst. Growth Des.* **2012**, *12*, 1830–1837. [[CrossRef](#)]
17. Niu, D.; Yang, J.; Guo, J.; Kan, W.; Song, S.; Du, P.; Ma, J. Syntheses, Structures, and Photoluminescent Properties of 12 New Metal-Organic Frameworks Constructed by a Flexible Dicarboxylate and Various N-Donor Ligands. *Cryst. Growth Des.* **2012**, *12*, 2397–2410. [[CrossRef](#)]
18. Tai, X.; Jie, Y. Synthesis, Crystal Structure and Antibacterial Activity of Mg(II) Complex $[Mg(H_2O)_6] \cdot (4\text{-amino-3-methylbenzenesulfonate})_2$. *Crystals* **2015**, *5*, 294–301. [[CrossRef](#)]
19. Tai, X.; Zhao, W. Synthesis, crystal structure, and antibacterial activity of magnesium (II) coordination polymers formed by hydrogen bonding. *Res. Chem. Intermed.* **2015**, *41*, 3471–3478. [[CrossRef](#)]
20. Ali, H.; Omar, S.N.; Drawsheh, M.D.; Fares, H. Synthesis, characterization and antimicrobial activity of zinc (II) ibuprofen complexes with nitrogen-based ligands. *J. Coord. Chem.* **2016**, *69*, 1110–1122. [[CrossRef](#)]
21. Jinu, U.; Gomathi, M.; Saiqa, I.; Geetha, N.; Benelli, G.; Venkatachalam, P. Green engineered biomolecule-capped silver and copper nanohybrids using *Prosopis cineraria* leaf extract: Enhanced antibacterial activity against microbial pathogens of public health relevance and cytotoxicity on human breast cancer cells (MCF-7). *Microb. Pathog.* **2017**, *105*, 86–95. [[CrossRef](#)] [[PubMed](#)]
22. Morgan, P.W.; Herr, B.C. Some dicarboxylic acids and esters containing the phosphine oxide group. *J. Am. Chem. Soc.* **1952**, *74*, 4526–4529. [[CrossRef](#)]
23. Bruker, S.M.A.R.T. *SAINT and SADABS*; Bruker AXS Inc.: Madison, WI, USA, 1998.
24. Sheldrick, G.M. *SHELXS-97, Program for X-ray Crystal Structure Determination*; University of Gottingen: Gottingen, Germany, 1997.
25. Sheldrick, G.M. *SHELXL-97, Program for X-ray Crystal Structure Refinement*; University of Gottingen: Gottingen, Germany, 1997.
26. Spek, A.L. *PLATON, A Multipurpose Crystallographic Tool*; Utrecht University: Utrecht, The Netherlands, 2002.
27. Zheng, J.Y.; Wang, G.B. *Medicines and Chemical Reagents Microbiology and Assay Technology*; People's Health Press: Beijing, China, 1989.
28. Allendorf, M.D.; Bauer, C.A.; Bhaktaa, R.K.; Houka, R.J.T. Luminescent metal-organic frameworks. *Chem. Soc. Rev.* **2009**, *38*, 1330–1332. [[CrossRef](#)] [[PubMed](#)]
29. Keypour, H.; Mahmoudabadi, M.; Shooshtari, A. Synthesis of Mn(II) and Zn(II) complexes with new macrocyclic Schiff-base ligands containing piperazine moiety: Spectroscopic, structural, cytotoxic and antibacterial properties. *Polyheron* **2017**, *127*, 345–354. [[CrossRef](#)]
30. Grabchev, I.; Yordanova, S.; Bosch, P.; Vasileva-Tonkov, E.; Kukeva, R.; Stoyanov, S.; Stoyanova, R. Structural characterization of 1,8-naphthalimides and in vitro microbiological activity of their Cu(II) and Zn(II) complexes. *J. Mol. Struct.* **2017**, *1130*, 974–983. [[CrossRef](#)]



© 2017 by the authors. Licensee MDPI, Basel, Switzerland. This article is an open access article distributed under the terms and conditions of the Creative Commons Attribution (CC BY) license (<http://creativecommons.org/licenses/by/4.0/>).